

Electroreduction of molecular oxygen on preferentially oriented platinum electrodes in acid solution

C. F. ZINOLA, A. M. CASTRO LUNA, W. E. TRIACA, A. J. ARVIA

Instituto de Investigaciones Fisicoquímicas Teóricas y Aplicadas, (INIFTA), Universidad Nacional de La Plata, Sucursal 4, Casilla de Correo 16, (1900) La Plata, Argentina

Received 3 November 1992; revised 7 April 1993

The oxygen electroreduction reaction was studied on two different preferentially oriented ((1 1 1)-type and (1 0 0)-type) and on a conventional polycrystalline (PC) platinum rotating disc electrodes in acid solutions at 30 °C. At low overpotentials, Tafel lines of $-0.060 \text{ V decade}^{-1}$ were obtained on the three electrodes in oxygen-saturated 1.0 M H_2SO_4 and 1.0 M $\text{H}_2\text{SO}_4 + y \text{ M K}_2\text{SO}_4$ ($0 \leq y \leq 1$). At high overpotentials the usual Tafel slope of $-0.120 \text{ V decade}^{-1}$ was observed on both (1 1 1)-type and PC platinum electrodes in 1.0 M H_2SO_4 , whereas a slope of $-0.165 \text{ V decade}^{-1}$ was found on (1 0 0)-type platinum. In oxygen-saturated 1.0 M H_2SO_4 the surface coverage by O-containing adsorbates on (1 0 0)-type platinum was greater than on both (1 1 1)-type and PC platinum. Rotating ring-disc electrode data showed that a higher amount of H_2O_2 was produced on (1 0 0)-type platinum than on the other platinum surfaces. The overpotential against current density plots are influenced by the anion concentration depending on the type of preferentially oriented platinum.

1. Introduction

The oxygen-electroreduction reaction deserves special attention because of its importance for metal corrosion in oxygen-containing solutions, air-metal batteries and fuel cells [1–6]. In the area of electrochemical energy conversion technology, platinum electrocatalysts are particularly vital for this reaction. Tafel plots for oxygen-electroreduction on smooth polycrystalline (PC) platinum in both diluted H_2SO_4 and HClO_4 exhibit a $-0.120 \text{ V decade}^{-1}$ slope at high current densities (c.d.), and a $-0.060 \text{ V decade}^{-1}$ slope at low c.d. The kinetics of the reaction has been explained in terms of the initial charge transfer step being rate-determining, assuming for the intermediates Temkin adsorption conditions at low c.d. and Langmuir adsorption conditions at high c.d. [7, 8]. On the other hand, the $-0.060 \text{ V decade}^{-1}$ slope at low c.d. has also been associated with a rate determining chemical step following the initial electron transfer [7]. Another possible reaction pathway comprising a set of parallel reactions involving two types of active sites with different adsorption energies, has been proposed [9]. Accordingly, adsorbed O-containing species could be desorbed easier from a certain type of sites by a direct electroreduction to H_2O through a 4-electron transfer reaction, or alternatively forming H_2O_2 , via a 2-electron transfer reaction, the latter further decomposing to H_2O . Otherwise, the kinetics of oxygen-electroreduction on PC platinum in H_3PO_4 solutions at different concentrations [10, 11], and in the presence of specifically adsorbed anions [12, 13], depends strongly on the anion concentration, particularly at high c.d. These effects were attributed to the

blockage of electroactive platinum sites by anion adsorption.

Studies of oxygen-electroreduction on both well-ordered low Miller index and stepped platinum surfaces in acid solutions [7, 14] suggested that there is no large influence of platinum surface structure on the kinetics of the reaction. However, it was recently [15] claimed that oxygen-electroreduction on Pt(1 1 1), Pt(1 0 0) and Pt(1 1 0) in 1.0 M H_2SO_4 , 1.0 M H_3PO_4 and 0.1 M $\text{HCl} + 1.0 \text{ M H}_2\text{SO}_4$ becomes a structure-sensitive reaction. Such results justify further work on this subject by using platinum electrodes whose surfaces were preferentially oriented either as (1 1 1)-type Pt or (1 0 0)-type Pt. The conclusions from this work can be correlated to those derived previously for platinum single crystal (SC) electrodes. The easy preparation and handling of these preferentially oriented surfaces, in addition to their stability during operation, are promising approaches for their applications in electrochemical devices [16].

2. Experimental details

Platinum discs (99.999% purity, 3 mm dia.) were used as working electrodes. The preparation of either (1 1 1)-type or (1 0 0)-type preferentially oriented platinum electrodes was made as described elsewhere [16]. For comparative purposes smooth PC platinum discs were occasionally employed. A large platinized-Pt plate (10 cm² of geometric area) counter electrode, facing the working electrode for minimizing ohmic drop effects, was used. A RHE in the same solution, connected to the rest of the cell through a Luggin-Haber capillary tip, was employed as reference elec-

trode. All potentials in the text are referred to the RHE scale. The real surface area of the working electrodes was estimated by comparing the H-atom voltammetric charge recorded at 0.1 V s^{-1} , to the H-atom monolayer charge density on the different oriented platinum surfaces [17].

Prior to the preparation of the preferentially oriented surfaces, the PC platinum discs were mechanically polished with different grades of alumina down to $0.05 \mu\text{m}$ grit, repeatedly rinsed with triply-distilled water, and finally, immersed for 1 h in the working electrolyte solution. The electrochemical behaviour of the preferentially oriented platinum electrodes was followed through the H and O-atom electroadsorption voltammograms at 0.1 V s^{-1} in $1.0 \text{ M H}_2\text{SO}_4$. SEM micrographs of the platinum surfaces were also made.

Measurements of the oxygen-electroreduction steady state potential against current density and of the surface coverage by O-containing adsorbates were determined in oxygen-saturated, ($P_{\text{O}_2} = 1 \text{ atm}$), $1.0 \text{ M H}_2\text{SO}_4 + y \text{ M K}_2\text{SO}_4$ ($0 \leq y \leq 1.0$). Solutions were prepared from Milli-Pore*-Milli-Q* water, 98% H_2SO_4 and anhydrous K_2SO_4 (Merck p.a.). The composition of the solutions used in the present work involves pH values in the 0.89–1.06 range, and $(\text{HSO}_4^-)/(\text{SO}_4^{2-})$ concentration ratios between 3.0 and 3.7 [18]. N_2 (99.99%) and O_2 (99.998%) were purified as indicated elsewhere [19].

All experiments were conducted at 30°C . Previously to each run a potential routine was applied to the working electrode to assure cleanness and reproducibility of the surface. It comprised a potential step at 1.4 V for 5 s to oxidize adsorbed impurities, followed by a potential step to 0.1 V for another 5 s to electroreduce the O-containing surface layer. The resulting prerduced platinum surface was employed to obtain the steady state potentiostatic polarization curves at 2000 r.p.m. by recording the current for various preset potentials in the 0.1 – 1.0 V range. Under these conditions the steady currents were attained after about 5 min.

The values of I_k , the net kinetic current, were derived from I , the experimental current, through the following equation:

$$I_k = \frac{I I_{\text{lim}}}{I_{\text{lim}} - I} \quad (1)$$

where $I_{\text{lim}}/(I_{\text{lim}} - I)$ is the diffusion contribution correction and I_{lim} is the observed limiting diffusion current.

A Tacussel rotating ring-disc electrode (RRDE) device was also used. The characteristics of the rotating electrode were $r_1 = 0.20 \text{ cm}$, $r_2 = 0.22 \text{ cm}$ and $r_3 = 0.24 \text{ cm}$, where r_1 is the radius of the disc, and r_2 and r_3 are the radii of the inner and the outer circles of the platinum ring electrode. The collection efficiency of the RRDE was 0.22.

The steady state coverage of the platinum electrode by O-containing surface species at different potentials was determined from q_0 , the charge density derived

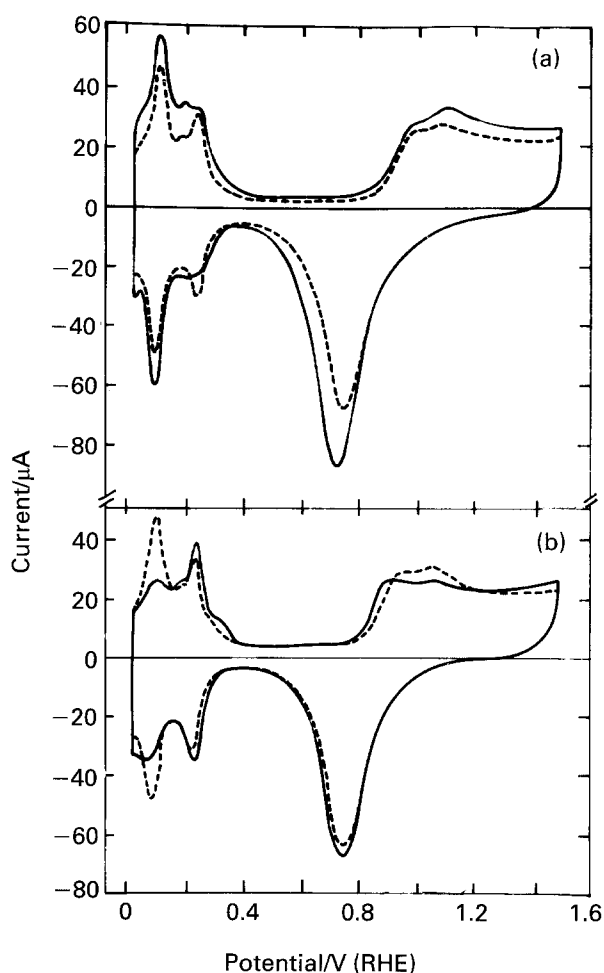


Fig. 1. Voltammograms run at 0.1 V s^{-1} in $1.0 \text{ M H}_2\text{SO}_4$ at 30°C . (---) untreated PC platinum; (—) (a) after 40 min SSWPP at 1.0 kHz between 0.60 and 1.45 V , real electrode area: 0.24 cm^2 ; (b) after 20 min SWPP at 1.0 kHz between 0.05 and 1.70 V , real electrode area: 0.22 cm^2 .

from the current transients recorded after applying a potential-step from the preset potential down to 0.3 V , i.e. a potential where the O-containing surface species are no longer preset. The fractional surface coverages by O-adatoms, θ_{O} , were calculated from the $q_{\text{O}}/2q_{\text{H}}$ ratio, where q_{H} denotes the H-atom monolayer charge density on each preferentially oriented surface [17].

3. Results

3.1. General behaviour of PC and preferentially oriented platinum surfaces

There are multiple states of adsorbed hydrogen at the PC platinum surface (starting material) as observed in the corresponding cyclic voltammograms of Fig. 1. The two principal current peaks are associated with H-adsorption on Pt (111) and Pt (110) facets (weakly adsorbed hydrogen), and Pt (100) facets (strongly adsorbed hydrogen). The distribution of different crystallographic facets is strongly dependent on the pretreatment of the PC platinum electrode. The percentage (in average) of distribution of strongly (s) and weakly (w) adsorbed-H at the starting PC plati-

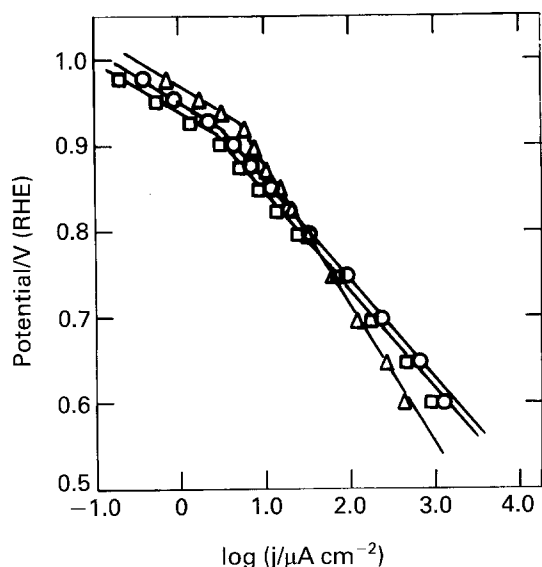


Fig. 2. Tafel lines for oxygen-electroreduction in oxygen-saturated 1.0 M H₂SO₄ at 30 °C for (□) PC; (Δ) (100)-type and (○) (111)-type platinum.

num follows the same trend than that previously reported for a high temperature treated PC platinum electrode [20, 21], that is, about 31% (*s*) and 53% (*w*).

The PC platinum electrode was subjected to a symmetric square wave periodic potential (SSWPP) between 0.60 and 1.45 V at 1.0 kHz for 40 min. The voltammetric response of the resulting new surface (Fig. 1(a)), hereafter denoted as (111)-type Pt, is similar to that reported previously for a platinum surface with a high proportion of reaction sites for weakly adsorbed H-atoms, and platinum single crystal stepped surfaces with (111) narrow terraces [22–24].

On the other hand, after the SSWPP treatment between 0.05 and 1.70 V at 1.0 kHz during 20 min., the voltammetric profile (Fig. 1(b)) of the treated surface, hereafter denoted as (100)-type Pt, approaches that

reported for platinum surfaces with a high proportion of reacting sites for strongly adsorbed hydrogen atoms, and platinum single crystal stepped surfaces with (100) narrow terraces [22, 23, 25].

SEM patterns of both (111)-type and (100)-type Pt electrodes exhibit the same typical faceted topography of each preferentially orientation already reported elsewhere [16, 22].

3.2. Tafel behaviour

The Tafel plots for oxygen-electroreduction on (111)-type Pt in oxygen saturated ($P_{O_2} = 1$ atm) 1.0 M H₂SO₄ at 30 °C show two straight line portions (Fig. 2). In the low overpotential region (l.o.r.) the value of the Tafel slope is $b_T = -0.067$ V decade⁻¹ and the value of the corresponding exchange current density is $j_0 = 3 \times 10^{-6}$ μA real cm⁻², whereas in the high overpotential region (h.o.r.), $b_T = -0.121$ V decade⁻¹, and $j_0 = 6.0 \times 10^{-3}$ μA real cm⁻² (Table 1). The same qualitative behaviour can be observed for (100)-type Pt (Fig. 2), but in this case, $b_T = -0.064$ V decade⁻¹ and $j_0 = 6 \times 10^{-6}$ μA cm⁻² in the l.o.r., and $b_T = -0.165$ V decade⁻¹ and $j_0 = 6.0 \times 10^{-2}$ μA cm⁻² in the h.o.r. It should be noted that the behaviour of PC platinum is similar to that of (111)-type Pt (Fig. 2). The Tafel lines for the three types of platinum exhibit a crossover point at about 0.92 V, i.e. in the potential region corresponding to the onset of OH irreversible adsorption [26], indicating a change in the kinetics of the electrode reaction.

3.3. The degree of surface coverage by O-containing species

The dependence of θ_O on the applied potential was

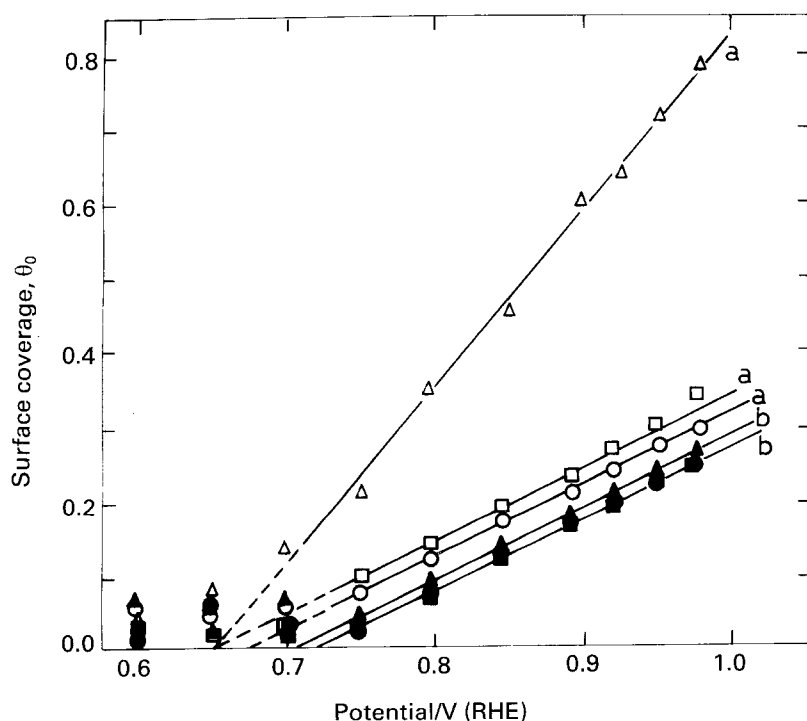


Fig. 3. Dependence of the surface coverage by O-containing species on electrode potential in oxygen-saturated, (a), and deoxygenated, (b), 1.0 M H₂SO₄ solutions at 30 °C. (a) (□) PC; (Δ) (100)-type and (○) (111)-type, (b) (■) PC; (▲) (100)-type and (●) (111)-type platinum.

Table 1. Oxygen-electroreduction kinetic parameters on preferentially oriented and PC platinum electrodes in different solutions, 30 °C.

Electrolyte	(111)-type Pt			PC Pt			(100)-type Pt							
	$-b_T/V \text{ dec}^{-1}$	$i_0/\mu\text{A cm}^{-2} \times 10^3$	$-b_T/V \text{ dec}^{-1}$	$i_0/\mu\text{A cm}^{-2} \times 10^3$	$-b_T/V \text{ dec}^{-1}$	$i_0/\mu\text{A cm}^{-2} \times 10^3$	$-b_T/V \text{ dec}^{-1}$	$i_0/\mu\text{A cm}^{-2} \times 10^3$						
	<i>h.o.r.</i>	<i>l.o.r.</i>	<i>h.o.r.</i>	<i>l.o.r.</i>	<i>h.o.r.</i>	<i>l.o.r.</i>	<i>h.o.r.</i>	<i>l.o.r.</i>						
1.0 M H ₂ SO ₄	0.121	0.067	0.067	6.0 ± 0.4	0.003 ± 0.001	0.125	0.070	5.0 ± 0.4	0.002 ± 0.0008	0.165	0.064	0.064	60.0 ± 0.1	0.006 ± 0.001
1.0 M H ₂ SO ₄ + 0.5 M K ₂ SO ₄	0.144	0.064	0.064	2.1 ± 0.1	0.002 ± 0.0008	0.140	0.068	4.0 ± 0.1	0.001 ± 0.0006	0.164	0.061	0.061	29.0 ± 0.2	0.002 ± 0.0008
1.0 M H ₂ SO ₄ + 1.0 M K ₂ SO ₄	0.164	0.065	0.065	0.9 ± 0.1	0.001 ± 0.0006	0.163	0.069	3.0 ± 0.1	0.0007 ± 0.0002	0.162	0.062	0.062	5.2 ± 0.1	0.001 ± 0.0006

determined in both oxygen-saturated and oxygen-free 1.0 M H₂SO₄ covering the 0.60–1.00 V range. For the three types of platinum the plots show almost linear θ_{O} against E dependences from 0.75 V up to 1.0 V (Fig. 3). For the (1 1 1)-type and PC platinum. In oxygen-saturated 1.0 M H₂SO₄ the slopes of the θ_{O} against E plots, are the same and equal to 0.85 V⁻¹, but their extrapolation to $\theta_{\text{O}} = 0$ yields $E_{\theta_{\text{O}}=0} = 0.67$ V for the (1 1 1)-type and $E_{\theta_{\text{O}}=0} = 0.65$ V for PC platinum. In this respect, the behaviour of (1 0 0)-type Pt is somewhat different, since all surface coverage values are much greater than those found on other platinum surfaces. In this case, the slope of the θ_{O} against E straight line is 1.13 V⁻¹ and $E_{\theta_{\text{O}}=0} = 0.65$ V. $E_{\theta_{\text{O}}=0}$ can be considered as the potential related to the hypothetical condition corresponding to $\theta_{\text{O}} = 0$. Values of θ_{O} for (1 0 0)-type Pt in oxygen-free 1.0 M H₂SO₄ are at each potential much lower than the corresponding ones found in the oxygen-saturated solution. Besides that, θ_{O} values for both (1 1 1)-type and PC platinum surfaces in the oxygen-free solution, are only slightly lower than those found for (1 0 0)-type Pt under the same experimental conditions.

3.4. Rotating ring-disc data

RRDE-voltammetry data obtained with preferentially oriented and PC platinum electrodes in oxygen-saturated 1.0 M H₂SO₄ are depicted in Fig. 4. In these runs the disc potential was scanned at 0.010 V s⁻¹ and the potential at the ring was held at 1.2 V, i.e. in the potential region where the diffusion controlled electrooxidation of H₂O₂ to O₂ takes place. Hence, the H₂O₂ produced during the oxygen-electroreduction at the disc electrode could be collected and detected at the ring electrode.

The ring current, I_{R} , against the disc potential, E_{D} , plots at $\omega = 2000$ r.p.m. for the three types of platinum electrodes show principally two peaked values of I_{R} , namely at about 0.40 V (peak I) and at about

0.18 V (peak II). A control experiment, run under nitrogen saturation, revealed that peaks I and II are exclusively recorded when the oxygen-electroreduction takes place. For (1 0 0)-type Pt there is a relatively large contribution of peak I which is shifted positively to about 0.44 V, whereas peak II is considerably diminished. On the other hand, peak I for both (1 1 1)-type and PC platinum is lower and shows a hump near 0.50 V.

3.5. Influence of the solution composition

The addition of K₂SO₄ to 1.0 M H₂SO₄ solution, changes the kinetic parameters resulting from the Tafel plots for the three types of platinum as shown in Table 1. Higher K₂SO₄ concentration increases the value of b_{T} at the h.o.r. for (1 1 1)-type and PC platinum in contrast to the invariant values of b_{T} found for (1 0 0)-type Pt which remain higher than the usual Tafel slope of -0.120 V decade⁻¹. Furthermore, the presence of K₂SO₄ in the electrolyte decreases the corresponding j_0 values for the three types of platinum in both Tafel regions. Since the changes in pH and (HSO₄⁻)/(S₄²⁻) equilibrium after addition of K₂SO₄ are not significant, the increase in the b_{T} value at the h.o.r. for both (1 1 1)-type and PC platinum must be principally attributed to the increase of the specific adsorption of anions. On the other hand, the (1 0 0)-type Pt is covered by a large amount of O-containing species, so there is practically no effect of the anionic adsorption on b_{T} in contrast to the decreasing value of j_0 as the K₂SO₄ concentration is increased.

Tafel plots were also obtained for the preferentially oriented platinum surfaces from current-potential curves run at 30 °C in weakly adsorbing media, namely, dilute H₂SO₄ and HClO₄ solutions. The corresponding kinetic parameters confirm the above mentioned trend. Thus, Tafel slopes of -0.120 V decade⁻¹ and -0.124 V decade⁻¹ were

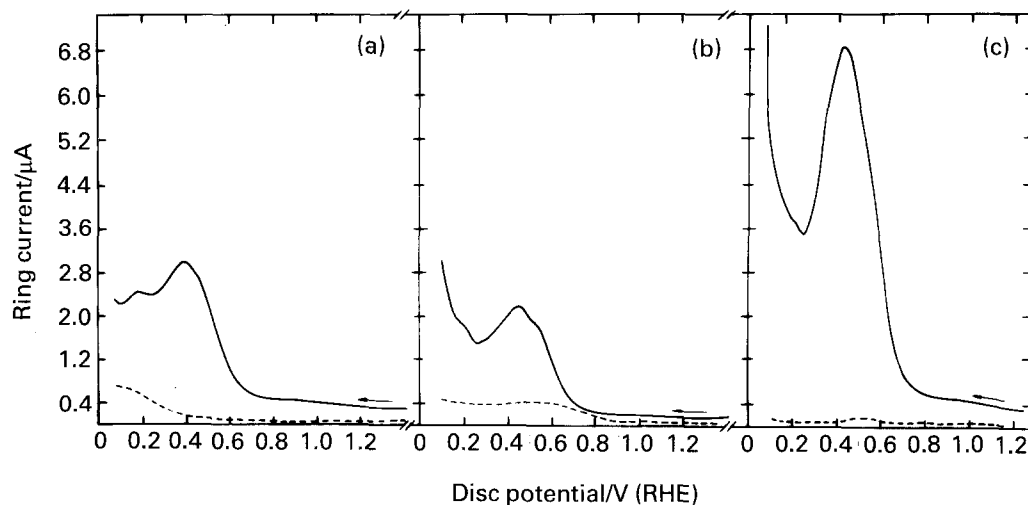


Fig. 4. Ring electrode current for hydrogen peroxide oxidation during oxygen-electroreduction in oxygen-saturated 1.0 M H₂SO₄ solution at 30 °C. The rotation speed was 2000 r.p.m. and the ring potential was held at 1.20 V. The arrows show the potential scan direction at the disc electrode; $v = 0.01$ V s⁻¹; (—) (a) PC Pt real electrode area: 0.13 cm², (b) (1 1 1)-type Pt real electrode area: 0.13 cm², (c) (1 0 0)-type Pt real electrode area: 0.12 cm². (- - -) runs in deoxygenated solution.

observed at the h.o.r. for (111)-type Pt in oxygen saturated 0.1 M H₂SO₄ and 0.1 M HClO₄ respectively, whereas a b_T value of $-0.136 \text{ V decade}^{-1}$, that is, a Tafel slope higher than $2.3(2RT/F)$, was found for (100)-type Pt in both electrolytes.

4. Discussion

The preceding results show that comparable values of b_T and j_0 are derived from the steady state oxygen-electroreduction Tafel plots on both PC and (111)-type Pt electrodes in 1.0 M H₂SO₄. The corresponding kinetic parameters (Table 1) are in part coincident with data reported earlier [8, 9, 27, 28]. The value $b_T = -0.120 \text{ V decade}^{-1}$, was interpreted through a mechanism involving the first single electron transfer as r.d.s. and Langmuir adsorption conditions for the reaction intermediates [7, 28]. Otherwise, the value $b_T = -0.060 \text{ V decade}^{-1}$ was associated with either a rate determining chemical step following the primary electron transfer [7] or the first electron transfer becoming r.d.s. under Temkin adsorption conditions for the O-containing surface intermediates [7, 8]. On the other hand, the results obtained on (100)-type Pt electrodes in 1.0 M H₂SO₄ show $b_T = -0.165 \text{ V decade}^{-1}$ in the h.o.r., i.e. a Tafel slope higher than $2.3(2RT/F)$, and the same $b_T = -0.060 \text{ V decade}^{-1}$ in the l.o.r., this behaviour being maintained in more dilute acid solutions, such as 0.1 M H₂SO₄ and 0.1 M HClO₄. Furthermore, Tafel slopes higher than $2.3(2RT/F)$ were also found at the h.o.r. on both (111)-type and PC platinum after addition of K₂SO₄ to the electrolyte solution.

Values of b_T higher than $2.3(2RT/F)$ for the oxygen-electroreduction on PC platinum in the h.o.r. were reported by Yeager *et al.* [10] and Glass *et al.* [12] in H₃PO₄ and in HCl-containing solutions [13, 15]. These values of b_T were explained through a blockage of platinum electroactive sites for the reaction by specifically adsorbed anions. As a first approach this explanation could be applied to the kinetics of the reaction in K₂SO₄ + H₂SO₄ solutions. On the other hand, interference by a differential anion adsorption in the electroreduction of hydrogen and oxygen adatoms on the platinum single crystal has also been reported [29, 30]. Tafel slopes for the oxygen-electroreduction on PC platinum higher than $-0.120 \text{ V decade}^{-1}$ were also found in the h.o.r. in alkaline solutions [31], and in this case H₂O₂ electrogeneration was demonstrated. It should also be noted that in H₃PO₄ solutions [10] about 10% of the overall oxygen electroreduction proceeds via H₂O₂. The RRDE data obtained in the present work on (100)-type Pt (Fig. 4) reveal, at the ring electrode, a current contribution due to the H₂O₂-electrooxidation higher than that found on either (111)-type or PC platinum. Accordingly, it appears that for (100)-type Pt the Tafel slope exceeding $2.3(2RT/F)$ is related to the fact that a part of the oxygen-electroreduction reaction is via H₂O₂, as it is detected at the ring electrode. Therefore, there are two reasonable explanations for the

values of b_T exceeding $-0.120 \text{ V decade}^{-1}$ based on a blockage effect, namely, the possible adsorption of either anions or peroxide species produced in the proper reaction.

The present results show that θ_O at constant potential, for (100)-type Pt in oxygen-free 1.0 M H₂SO₄, is slightly higher than that found on either (111)-type or PC platinum. The values of θ_O for the latter coincide with those previously reported by different authors [7, 28, 32, 33]. This fact agrees with the higher voltammetric charges found for the O-electrosorption on Pt (100) as compared to Pt (111) and Pt (110) single crystals [15]. On the other hand, the present results indicate that θ_O values for (100)-type Pt in oxygen-containing solution are much greater than in oxygen-free solution. Thus, at 0.97 V for (100)-type Pt in oxygen-saturated 1.0 M H₂SO₄, $\theta_O = 0.78$, whereas in the oxygen-free 1.0 M H₂SO₄ $\theta_O = 0.28$. It should be noted that according to the preceding analysis θ_O may actually involve two O-adsorbed species, one resulting from the upd discharge of water, the other produced from the oxygen-electroreduction intermediates. It is likely that larger contributions of O-adsorbed electroactive intermediates, such as peroxide species, are particularly involved on (100)-type Pt in the oxygen-saturated acid solution.

The values of j_0 resulting from the extrapolation of the h.o.r. linear Tafel region to the $E_r(\text{O}_2/\text{H}_2\text{O}) = 1.23 \text{ V}$ for (100)-type Pt, are one order of magnitude higher than those resulting for other platinum electrodes. On the other hand, the values of j_0 obtained for PC and (111)-type Pt are in good agreement with those already reported for PC platinum by Damjanovic *et al.* in H₂SO₄ solution at pH 1.9 [8], and by Yeager *et al.* [10] in 85.5% H₃PO₄ at 25 °C.

The presence of a high concentration of adsorbable anions, such as SO₄²⁻ and HSO₄⁻ (Table 1), tends to hinder the adsorption of O-containing species produced in the oxygen-electroreduction reaction through a competitive adsorption at platinum electroactive sites. In this respect, the tetrahedral structures of SO₄²⁻ and HSO₄⁻ favour their adsorption on surfaces with the (111) trigonal symmetry [34]. This fact correlates with the increase of b_T with the anion concentration at the h.o.r. on (111)-type Pt (Table 1). In contrast, when the structural coupling is not facilitated weaker adsorption effects on the kinetics of the reaction are expected. This is apparently the case for SO₄²⁻ and HSO₄⁻ on (100)-type Pt. The mismatch of the corresponding geometries helps to produce a cathodic shift of the O-electrosorption potential range as compared to (111)-type Pt. This is confirmed by the O-electrosorption voltammetric profiles of the different preferentially oriented surfaces (Fig.1).

The preceding explanation is consistent with the conclusions of Angerstein-Kozłowska *et al.* [35] that the presence of specifically adsorbed anions produces a dual effect on the O-electrosorption, namely, a

potential dependent blockage of surface sites and a shift of the O-electroadsorption potential range [36] due to the changes on the local field by adsorbed anions. When the oxygen-electroreduction is carried out on an oxidized platinum electrode, oxygen molecules cannot bond strongly to the surface, because a large number of the platinum sites are covered by O-adsorbed atoms. In this case, the free energy of adsorption of the oxygen molecules is not large enough to break the O–O bond and, consequently, the most probable mechanism for the reaction is a 2-electron path yielding H₂O₂ [37]. On the other hand, it is known that the amount of H₂O₂ detected at the ring electrode in 0.1 M NaOH increases with the degree of oxidation of the platinum disc surface, as described by Luk'yanycheva *et al.* [38]. The O-electroadsorption region appearing at lower potentials on the (100)-type Pt electrode and the higher amounts of H₂O₂ generated from this type of surface, are in accordance with the above considerations.

At potentials more positive than 0.9 V (vs RHE), anions tend to desorb as a result of their competition with O-containing species [39, 40]. Accordingly, the values of b_T tend to coincide for the different platinum electrodes. This is shown through the steady state Tafel plots on the preferentially oriented Pt surfaces in H₂SO₄ solutions containing different amounts of K₂SO₄, whose kinetic parameters are given in Table 1.

5. Conclusions

(i) The oxygen-electroreduction kinetics on (111)-type Pt electrodes in acid media is found to be similar to that reported by many authors for smooth PC platinum.

(ii) Through the specific blockage of the electrode surface, the oxygen-electroreduction behaves as a surface structure-sensitive reaction in the h.o.r.

(iii) The blockage effect can be attributed to the presence of adsorbable anions and to the formation of peroxide species in the oxygen-electroreduction.

(iv) Results suggest that the surface blockage by SO₄²⁻ and HSO₄⁻ anions is favoured on (111)-type Pt, whereas peroxide species are mainly responsible for the (100)-type Pt blockage.

Acknowledgements

This work was financially supported by the Universidad Nacional de La Plata, the Consejo Nacional de Investigaciones Científicas y Técnicas, the Comisión de Investigaciones Científicas (Provincia de Bs. As.) and the Organization of American States. A.M.C.L. is a researcher of CIC. C.F.Z. thanks the Organization of American States and the Universidad de la República of Uruguay for the fellowship granted.

References

[1] M. R. Tarasevich, A. Sadkowsky and E. B. Yeager, in 'Comprehensive Treatise of Electrochemistry', (edited by J.

- O'M. Bockris, E. B. Yeager, S. U. M. Kahn and R. E. White), Vol. 7, Plenum Press, New York (1983) Chap. 6, p. 301.
- [2] J. P. Hoare, 'The Electrochemistry of Oxygen', Interscience, London-New York (1968) Chap. 4, p. 117.
- [3] E. B. Yeager, in 'Electrocatalysis on Non-Metallic Surfaces', NBS Special Publication 455 (1976) pp. 203–19.
- [4] A. J. Appleby, in 'Modern Aspects of Electrochemistry' (edited by J. O'M. Bockris and B. E. Conway), Vol. 9, Plenum Press (1974) p. 369.
- [5] M. W. Breiter, 'Electrochemical Processes in Fuel Cells', Springer-Verlag, New York (1969) Chap IX, p. 185.
- [6] B. V. Tilak, R. S. Yeo, S. Srinivasan, in 'Comprehensive Treatise of Electrochemistry' (edited by J. O'M. Bockris, B. E. Conway, E. B. Yeager and R. E. White) Vol. 3, Plenum Press, New York (1981) Chap. 2, p. 39.
- [7] A. Damjanovic and V. Brusic, *Electrochim. Acta* **12** (1967) 615.
- [8] D. B. Šepa, M. V. Vojnovic and A. Damjanovic, *ibid.* **26** (1981) 781.
- [9] E. B. Yeager, *ibid.* **29** (1984) 1527.
- [10] J. C. Huang, R. K. Sen and E. B. Yeager, *J. Electrochem. Soc.* **126** (1979) 786.
- [11] K. L. Hsueh, E. R. González and S. Srinivasan, *ibid.* **131** (1984) 822.
- [12] J. T. Glass, L. L. Cahen Jr. and G. E. Stoner, *ibid.* **136** (1989) 656.
- [13] S. M. Kaska, S. Sarangapani and J. Giner, *ibid.* **136** (1989) 75.
- [14] P. N. Ross Jr., *ibid.* **126** (1979) 78.
- [15] F. El Kadiri, R. Faure and R. Durand, *J. Electroanal. Chem.* **301** (1991) 177.
- [16] W. E. Triaca, T. Kessler, J. C. Canullo and A. J. Arvia, *J. Electrochem. Soc.* **134** (1987) 1165.
- [17] H. Angerstein-Kozłowska, in 'Comprehensive Treatise of Electrochemistry', (edited by E. B. Yeager, J. O'M. Bockris, B. E. Conway and S. Sarangapani), Vol. 9, Plenum Press, New York (1984) Chap. 2, pp. 15–61.
- [18] H. S. Harned and B. B. Owen, 'The Physical Chemistry of Electrolytic Solutions', American Chemical Society Monographs, 2nd edn, Reinhold, New York (1950) Chap. 14, pp. 445–80.
- [19] G. Brauer, 'Handbuch der Präparativen Anorganischen Chemie', Part I, Verlag, Stuttgart (1960) p. 304.
- [20] D. Armand and J. Clavilier, *J. Electroanal. Chem.* **225** (1987) 205.
- [21] *Idem ibid* **233** (1987) 251.
- [22] A. Visintín, A. J. Canullo, W. E. Triaca and A. J. Arvia, *ibid.* **239** (1988) 67.
- [23] A. V. Tripkovic and R. R. Adzic, *ibid.* **205** (1986) 335.
- [24] N. Furuya and S. Koide, *Surf. Sci.* **220** (1989) 18.
- [25] J. Clavilier, R. Durand, G. Guinet and R. Faure, *J. Electroanal. Chem.* **127** (1981) 281.
- [26] H. Angerstein-Kozłowska, B. E. Conway and W. B. A. Sharp, *ibid.* **43** (1973) 9.
- [27] A. J. Appleby, *ibid.* **24** (1970) 97.
- [28] H. Wroblowa, M. L. B. Rao, A. Damjanovic and J. O'M. Bockris, *ibid.* **15** (1967) 139.
- [29] E. K. Krauskopf, L. M. Rice and A. Wieckowski, *ibid.* **244** (1988) 347.
- [30] P. W. Faguy, N. Markovic, R. R. Adzic, C. A. Fierro and E. B. Yeager, *J. Electroanal. Chem.* **289** (1990) 245.
- [31] S. M. Park, S. Ho, S. Aruliah, M. F. Weber, C. A. Ward, R. D. Venter and S. Srinivasan, *J. Electrochem. Soc.* **133** (1986) 164.
- [32] V. A. Gromyko, Yu. B. Vasil'ev and V. S. Bagotskii, *Elektrokhimiya* **8** (1972) 914.
- [33] M. R. Tarasevich, *ibid.* **9** (1973) 599.
- [34] N. M. Markovic, N. S. Marinkovic and R. R. Adzic, *J. Electroanal. Chem.* **241** (1988) 309.
- [35] H. Angerstein-Kozłowska, B. E. Conway, B. Barnett and J. Mozota, *ibid.* **100** (1979) 417.
- [36] R. O. Lezna, N. R. de Tacconi and A. J. Arvia, *J. Electrochem. Soc.* **126** (1979) 2140.
- [37] J. P. Hoare, *Electrochim. Acta* **20** (1975) 267
- [38] V. I. Luk'yanycheva, A. Yuzhanina, M. R. Tarasevich, N. A. Shumilova and V. S. Bagotskii, *Elektrokhimiya* **13** (1977) 506.
- [39] V. E. Kazarinov and N. A. Baloshova, *Dokl. Fis. Chem.* **157** (1964) 795.
- [40] F. C. Nard and T. Iwasita, *J. Electroanal. Chem.* **308** (1991) 277.